Z. Phys. C – Particles and Fields 47, 343–351 (1990)

Zeitschrift für Physik C Particles and Fields
© Springer-Verlag 1990

Measurement of resonance production in the reactions $\gamma\gamma \to \pi^0\pi^0$ and $\gamma\gamma \to \pi^0\eta$

JADE Collaboration

T. Oest[2], J. Olsson[1], J. Allison[5], K. Ambrus[3,a], R.J. Barlow[5], W. Bartel[1], S. Bethke[3], C.K. Bowdery[4], S.L. Cartwright[7,b], J. Chrin[5], D. Clarke[7], A. Dieckmann[3], I.P. Duerdoth[5], G. Eckerlin[3], E. Elsen[3], R. Felst[1], A.J. Finch[4], F. Foster[4], T. Greenshaw[2], J. Hagemann[2,c], D. Haidt[1], J. Heintze[3], G. Heinzelmann[2], K.H. Hellenbrand[3,d], P. Hill[6,e], G. Hughes[4], H. Kado[1,f], K. Kawagoe[8], C. Kleinwort[2,c], G. Knies[1], S. Komamiya[3,g], H. Krehbiel[1], J. v. Krogh[3], M. Kuhlen[2,h], F.K. Loebinger[5], A.A. Macbeth[5], N. Magnussen[1,i], R. Marshall[7], R. Meinke[1], R.P. Middleton[7], P.G. Murphy[5], B. Naroska[2], J.M. Nye[4,j], F. Ould-Saada[2], D. Pitzl[2,k], R. Ramcke[1,l], H. Rieseberg[3], A. Sato[8], D. Schmidt[1,i], L. Smolik[3], U. Schneekloth[2,m], J.A.J. Skard[6,n], J. Spitzer[3], P. Steffen[1], K. Stephens[5], T. Takeshita[8], A. Wagner[3], I.W. Walker[4], G. Weber[2], M. Zimmer[3], G.T. Zorn[6]

[1] Deutsches Elektronen-Synchrotron DESY, D-2000 Hamburg, Federal Republic of Germany
[2] II. Institut für Experimentalphysik der Universität Hamburg, D-2000 Hamburg, Federal Republic of Germany
[3] Physikalisches Institut der Universität Heidelberg, D-6900 Heidelberg, Federal Republic of Germany
[4] University of Lancaster, Lancaster, England
[5] University of Manchester, Manchester, England
[6] University of Maryland, College Park, MD, USA
[7] Rutherford Appleton Laboratory, Chilton, Didcot, England
[8] International Center for Elementary Particle Physics, University of Tokyo, Tokyo, Japan

Received 6 April 1990

Abstract. Resonance production in the $\gamma\gamma$ reactions $e^+e^- \to e^+e^-\pi^0\pi^0$ and $e^+e^- \to e^+e^-\pi^0\eta$ has been studied with the JADE detector at PETRA. The decay widths into $\gamma\gamma$ of the $f_2(1270)$, $a_0(980)$ and $a_2(1320)$ were measured to be $\Gamma_{\gamma\gamma}(f_2(1270)) = 3.19 \pm 0.09^{+0.22}_{-0.38}$ keV, $\Gamma_{\gamma\gamma}(a_0(980)) = 0.28 \pm 0.04 \pm 0.10$ keV/BR$(a_0(980) \to \pi^0\eta)$ and $\Gamma_{\gamma\gamma}(a_2(1320)) = 1.01 \pm 0.14 \pm 0.22$ keV. For the $f_0(975)$ and $f_4(2050)$ upper limits of the widths were obtained, $\Gamma_{\gamma\gamma}(f_0(975)) < 0.6$ keV and $\Gamma_{\gamma\gamma}(f_4(2050)) < 1.1$ keV, both at the 95% C.L. Assuming that the spin 0 background under the $f_2(1270)$ is small, the $f_2(1270)$ was found to be produced exclusively in a helicity 2 state. The helicity 0 contribution is <15% at the 95% C.L. The cross section for $\gamma\gamma \to \pi^0\pi^0$ in the mass range 2.0–3.5 GeV/c^2 was measured for the first time. Since the cross section for $\gamma\gamma \to \pi^+\pi^-$ is a factor ~2 larger, $\pi\pi$ production in this range can be interpreted as taking place via isospin 0 production.

[a] Now at MBB, Munich, FRG
[b] Now at Sheffield University, Sheffield, UK
[c] Now at CERN, Geneva, Switzerland
[d] Now at Universität des Saarlandes, Saarbrücken, FRG
[e] Now at DESY, Hamburg, FRG
[f] Now at Bayer AG, Brunsbüttel, FRG
[g] Now at SLAC, California, USA
[h] Now at CALTECH, California, USA
[i] Universität-Gesamthochschule Wuppertal, Wuppertal, FRG
[j] Now at ESTEC, Noordwijk, The Netherlands
[k] Now at Santa Cruz, California, USA
[l] Now at Ramcke Datentechnik GmbH, Hamburg, FRG
[m] Now at MIT, Cambridge, Massachusetts, USA
[n] Now at ST Systems Corporation, Lanham, Maryland, USA

Introduction

Exclusive resonance production in $\gamma\gamma$ reactions has played an important role in the study of the electric charge of the sub-structure of resonances. The measurement of the decay widths into $\gamma\gamma$ allows one to test the predicted quark composition of the resonances and in this way provides a better understanding of the meson spectrum. So far, the best description of this spectrum is given by the naive $q\bar{q}$ model, but other models exist, in which meson states containing gluons, e.g. $q\bar{q}g$ or ggg, as well as multi quark states $qq\bar{q}\bar{q}$ are predicted.

Two candidates for $qq\bar{q}\bar{q}$ states are the $f_0(975)$ and the $a_0(980)$, both having quantum numbers $J^{PC} = 0^{++}$. The $f_0(975)$ is an isospin singlet and decays predominantly into $\pi\pi$, while the $a_0(980)$ is an isospin triplet with major decay mode $\pi\eta$. In the $q\bar{q}$ model these mesons constitute the ground states of the well known 2^{++} mesons $f_2(1270)$ and $a_2(1320)$, which appear in the same

decay channels. While the 2^{++} tensor states are well described in the $q\bar{q}$ model this is not the case for the scalar mesons $f_0(975)$ and $a_0(980)$, which have much smaller total widths than predicted.

In this paper we report on a study of the $\gamma\gamma$ reaction

$$e^+e^- \to e^+e^-\gamma\gamma\gamma\gamma, \tag{1}$$

and especially on the measurement of resonance production in the two processes

$$\gamma\gamma \to \pi^0\pi^0 \to \gamma\gamma\gamma\gamma, \tag{2}$$

$$\gamma\gamma \to \pi^0\eta \to \gamma\gamma\gamma\gamma. \tag{3}$$

Since the scattered electrons in general remain in the beampipe (no-tag events), the detected final state consists only of the four photons. The study of the decay mode $\pi^0\pi^0$, though more difficult to trigger and reconstruct than the charged mode $\pi^+\pi^-$, has the advantage that background from QED-processes ($\gamma\gamma \to e^+e^-, \gamma\gamma \to \mu^+\mu^-$) is negligible and background from direct $\pi\pi$ production is very low.

Another interesting subject which will be studied in the reaction $\gamma\gamma \to \pi^0\pi^0$ is the mass range beyond the $f_2(1270)$ resonance. Calculations in the framework of QCD [1, 2] give predictions on the shape and the size of the cross section, for both neutral and charged pion pair production. The measurement of these cross sections is an important check of these calculations. So far only charged pion pair production has been studied in this range [3]. In the present paper cross sections for $\gamma\gamma \to \pi^0\pi^0$ in the range 2.0–3.5 GeV/c^2 are given for the first time.

Detector and trigger

The measurements were performed with the JADE detector at the PETRA e^+e^- storage ring. The integrated luminosity was 149 pb^{-1}, obtained at an average beam energy of 18 GeV.

The JADE detector has been described in detail elsewhere [4]. Here we mention only those features of the detector that were essential to the present analysis. Of particular importance were the ability of the apparatus to detect and measure low energy photons and to trigger on final states with low visible energy, since in most cases the scattered electrons in reaction (1) escape into the beam pipe and are not detected. The final state photons in reactions (2) and (3) are all of fairly low energies, in the resonance region typically a few hundred MeV.

Photons were detected in the array of 2712 lead glass Čerenkov counters located behind the central jet chamber and the magnetic coil. A barrel section and two end cap sections furnished a solid angle coverage of 90%, with the barrel part subtending $|\cos\theta| < 0.82$ and the endcap parts covering $0.89 < |\cos\theta| < 0.97$; θ is the polar angle with respect to the beam. The barrel counters were arranged in 84 rows parallel to the beam, each with 30 counters, while the endcaps consisted of 96 counters each, arranged in 4 quadrants of 24 counters. The practical lower limit for detectable photon energies was ~40–50 MeV, given by the readout threshold of the lead glass counter electronics. The energy resolution, as determined from the measured width of the π^0 signal, varied between 25 and 10% for photon energies from 100–700 MeV, while the angular resolution was $\sigma_\phi \sim \sigma_\theta \sim 25$ mrad at these energies.

Another means of detecting photons was via the reconstruction of conversions into e^+e^- pairs. This was possible if the photons converted before or inside the central jet chamber.

Here the lower limit for detectable photon energies was given by the efficiency of the charged track pattern recognition program for the inner detector (the lower limit on the detectable track momentum was ~30 MeV/c).

The trigger for reaction (1) was based on linear energy sums ("septants") formed for 7 non-overlapping azimuthal regions of the barrel lead glass array. These consisted of 360 barrel counters and covered 12 rows with a corresponding azimuthal angle of 52°. In addition the array of 42 time of flight (TOF) scintillation counters situated outside the inner detector and inside the coil was used for the trigger.

Two trigger modes contributed to the event sample of reaction (1). In both modes, a coincidence of 2 roughly opposite septants was required (e.g. 1–4, 1–5, 2–5, etc. ...), with the measured energy sum exceeding in both septants the threshold of ~150 MeV. In the first trigger mode, no signal in the TOF counters was required. In this mode, all 4 photons of reaction (1) were detected in the leadglass. In the second mode, at least 1 (and <7) set TOF counter was required, together with at least 1 track in the inner detector track trigger logic. Events with converted photons were triggered in this mode.

The threshold behaviour of the septant energy sums as a function of the deposited energy was important since most events of reaction (1) are close to the energy threshold. Efficiency curves of the trigger as a function of deposited energy in the septants were obtained using events triggered in other, independent ways. These curves were used in the Monte Carlo simulation of reactions (2) and (3) to determine the trigger efficiency as is discussed below.

Event selection

To select events for reaction (1), the following criteria were used:

- The events were required to contain exactly 4 photons. A photon was defined to be either a reconstructed e^+e^- conversion or an energy cluster in the lead glass array to which no charged tracks could be associated. Clusters consisting of only one lead glass counter were required to have at least 45 MeV deposited energy (endcap clusters) or at least 50 MeV reconstructed photon energy (barrel clusters)*.

* Due to several corrections, e.g. for shower absorption or for differences in light attenuation at different angles of incidence, the reconstructed photon energy is in general different from the deposited cluster energy

• Apart from possible conversion e^+e^- pairs, the events should not contain other charged tracks. A track was required to have at least 8 measured points, to originate in a fiducial cylinder around the interaction point with radius 40 mm and length ± 200 mm and to have a transverse momentum with respect to the beam of at least 30 MeV/c. Thus, events with "curling" electrons from conversions, where the pattern recognition program found additional tracks either originating outside the fiducial region or having too low momentum or too few hits, were still included in the sample.

A total of 74662 events passed these criteria. Further cuts were applied to remove the most common background events:

• Converted photons were required to have the projected intersection point with the beam axis within ± 150 mm of the interaction point. In Fig. 1 the distribution of the projected z-vertex of converted photons is shown. A clear peak around the interaction point is seen. Note that this distribution at the same time provides clear evidence for the origin of the events in the beam-beam interactions.

• In events with several neighbouring lead glass clusters and no conversions, it was required that the photons be spread over an azimuthal range of at least 120°. This cut reduces background from cosmic rays which penetrate the lead glass system but do not give recognized tracks in the inner detector.

Finally, since photons detected in the endcap lead glass counters had worse angular and energy resolution, events with any such photon were rejected. The remaining events were visually inspected with help of a graphics program and background events, mainly from cosmic muons and from electronic noise, were rejected. After this selection 5722 events remained.

In Fig. 2 the correlation plot $m(\gamma_i\gamma_j)$ vs. $m(\gamma_k\gamma_l)$, $i,j,k,l=1\ldots4$ is shown, both for the 4γ mass (W) region 0.8–2.0 GeV/c^2 (Fig. 2a) and for $W>2.0$ GeV/c^2 (Fig. 2b). Three different combinations per event enter into the plots. In both W regions a clear $\pi^0\pi^0$ signal is seen; in addition in Fig. 2a $\pi^0\eta$ correlation is apparent. The broad distribution at higher $\gamma\gamma$ masses is due to the wrong $\gamma\gamma$ combinations from the $\pi^0\pi^0$ events.

The candidate $\pi^0\pi^0$ events were selected in the correlation plot by requiring at least one entry in a circular area (indicated in Fig. 2a) with radius 55 MeV/c^2 around the nominal $\pi^0\pi^0$ mass point. For events with more than one entry in this area, the combination with minimal

$$\chi^2_{\pi^0\pi^0}=\frac{(m_{\pi^0}-m_{\gamma_1\gamma_2})^2}{\sigma^2_{m_{\gamma_1\gamma_2}}}+\frac{(m_{\pi^0}-m_{\gamma_3\gamma_4})^2}{\sigma^2_{m_{\gamma_3\gamma_4}}} \quad (4)$$

was selected. The errors of the masses in (4) were calculated from the energy and angular resolution of each photon. Finally, each $\gamma\gamma$ pair was subjected to a constrained fit to the π^0 mass.

The candidate $\pi^0\eta$ events were selected in a similar way, by requiring at least one entry in an elliptically shaped area (indicated in Fig. 2a) with maximum deviations from the nominal π^0 and η masses of ± 55 and ± 150 MeV/c^2 respectively. To reject the background of wrong combinations from $\pi^0\pi^0$ events the $\chi^2_{\pi^0\pi^0}$ was calculated as described above for all possible $\pi^0\pi^0$ hypotheses. All events with a corresponding maximum $\pi^0\pi^0$ probability of more than 0.2% were rejected. This value was determined from a comparison with a Monte Carlo event simulation. If there were more than one entry in the $\pi^0\eta$ mass region, a $\chi^2_{\pi^0\eta}$ analogous to (4) was defined and the combination which minimized this quantity was

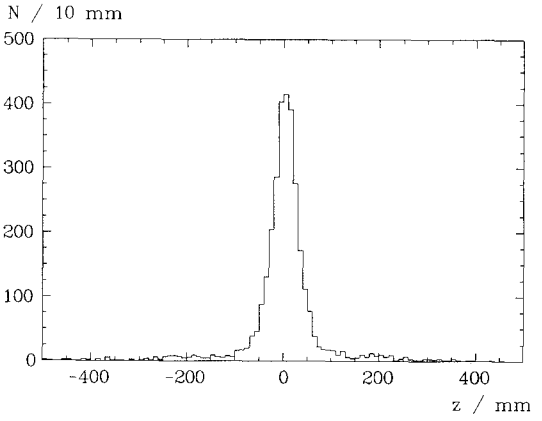

Fig. 1. Projected intersection point with the beam axis for converted photons.

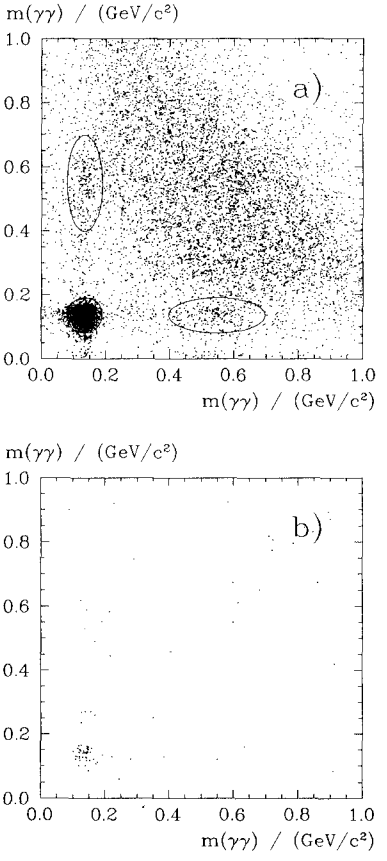

Fig. 2a, b. Mass($\gamma_1\gamma_2$) vs. mass($\gamma_3\gamma_4$), 3 entries/event. **a** $W=0.8-2.0$ GeV/c^2. **b** $W>2.0$ GeV/c^2

selected. Finally constrained fits to the π^0 and η masses were performed.

To reject background from non exclusive events (i.e. events with additional, undetected particles) and to restrict the photon Q^2 range to small ("quasi real") values, cuts in acoplanarity and transverse momentum p_t were applied. For $\pi^0\pi^0$ candidate events, the cuts were $\cos\phi < -0.9$ and $p_t < 250$ MeV/c; for $\pi^0\eta$ events, $\cos\phi < -0.8$ and $p_t < 250$ MeV/c, where ϕ is the angle in the plane perpendicular to the beam axis, either between the two π^0's or between the π^0 and the η. p_t is the net transverse momentum of the event with respect to the beam, obtained from the vector sum of the individual π^0 and η transverse momenta. After these cuts $2764\,\pi^0\pi^0$ and $291\,\pi^0\eta$ events remained.

Analysis of $\pi^0\pi^0$ and $\pi^0\eta$ resonance production

Figures 3 and 4 show the invariant mass distributions of the selected $\pi^0\pi^0$ and $\pi^0\eta$ events. Clear signals at the $f_2(1270)$, $a_0(980)$ and $a_2(1320)$ masses are seen. In addition, in Fig. 3 there is a small shoulder at

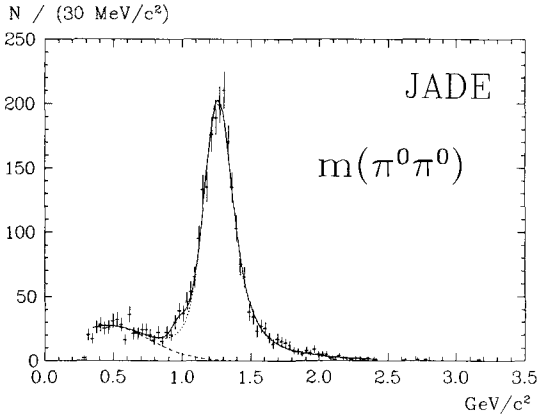

Fig. 3. Mass($\pi^0\pi^0$). The full curve shows a fit with a background term and two Breit-Wigner functions, for $f_0(975)$ and $f_2(1270)$. The dotted curve indicates the contribution from the $f_0(975)$ resonance, the dashed curve shows the background

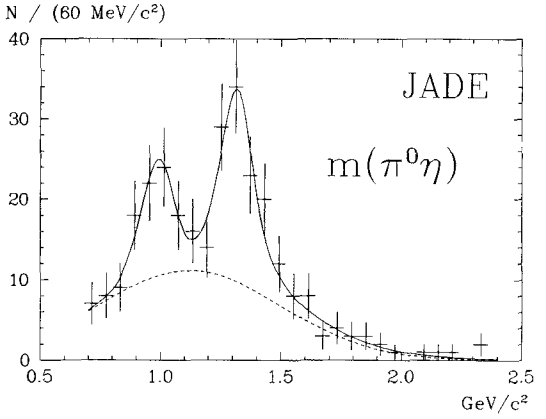

Fig. 4. Mass($\pi^0\eta$). The full curve shows a fit with a background term and two breit-Wigner functions, for $a_0(980)$ and $a_2(1320)$. The dashed curve shows the background

~ 1 GeV/c^2, which may come from the production of the $f_0(975)$. The statistical significance of the latter signal is $\sim 2\sigma$.

The cross section, $\sigma_{\gamma\gamma}$, for $\gamma\gamma$ production of a resonance R with spin J can be described by a Breit-Wigner function [5]

$$\sigma_{\gamma\gamma} = 8\pi(2J+1)\frac{\Gamma_R(W)\,\Gamma_{\gamma\gamma}}{(W^2-M_R^2)^2+\Gamma_R^2(W)\,M_R^2}, \tag{5}$$

where M_R is the resonance mass and $\Gamma_{\gamma\gamma}$ the decay width into two photons. In the parameterization of the energy-dependent width $\Gamma_R(W)$ [14, 15],

$$\Gamma_R(W) = \Gamma_0\left(\frac{|\mathbf{k}^*|}{|\mathbf{k}_0^*|}\right)^{2J+1}\frac{D_J(x_0)}{D_J(x)}, \tag{6}$$

$\mathbf{k}_0^*$ is the momentum of a decay particle in the resonance rest system at the nominal mass of the resonance, while $\mathbf{k}^*$ is the corresponding momentum at the invariant mass W. The spin-barrier factor $D_J(x)$, where $x = r|\mathbf{k}^*|$, is derived from a model of scattering on a constant potential with radius r [15, 16]. The $D_J(x)$ are given by the spherical Hankel functions [17], $D_J(x) \propto x^{2J+2}|h_J^{(1)}(x)|^2$, or, explicitly, $D_0(x) = 1$, $D_2(x) = x^4 + 3x^2 + 9$.

Helicity structure

In the presently considered restricted Q^2 range, only transversely polarized photons contribute to the cross section. Resonances are then produced in states of either helicity 0 or helicity 2. Restricting ourselves to spin 0 and 2 for masses below the lightest spin 4 resonance at about 2 GeV/c^2, the angular distribution of the decay into spin 0 stable particles can be written as

$$\frac{d^2\sigma_{\gamma\gamma}}{d\phi^* d\cos\theta^*} \propto G(\phi^*, \cos\theta^*) = |a'\,Y_2^2 + b'\,Y_2^0 + c'\,Y_0^0|^2, \tag{7}$$

where ϕ^* and θ^* are the angles of a decay particle with respect to the $\gamma\gamma$ axis, a', b', c' are constants and $Y_l^{l_z}$ spherical harmonics. Since we are dealing with untagged events and ϕ^* is not measured, (7), after integration over ϕ^*, leads to

$$G(\cos\theta^*) = a^2|Y_2^2|^2 + b^2|Y_2^0|^2 + c^2|Y_0^0|^2 + 2bc\,Y_2^0\,Y_0^0\cos\delta. \tag{8}$$

Here δ is the relative phase between Y_2^0 and Y_0^0 and the real parameters a, b, c give the relative contributions of the spin 2, helicity 2 and 0 and spin 0 components.

Since no explicit ϕ^* dependence appears in (8), a problem arises in the angular analysis. Although a comparison with data would seemingly allow the determination of the quantities a, b, c and δ, the linear dependence of the spherical harmonics,

$$\sqrt{6}|Y_2^2| = |Y_2^0 - \sqrt{5}\,Y_0^0|, \tag{9}$$

allows b, c and δ to be chosen such that a vanishes. Thus any helicity 2 component can always be expressed

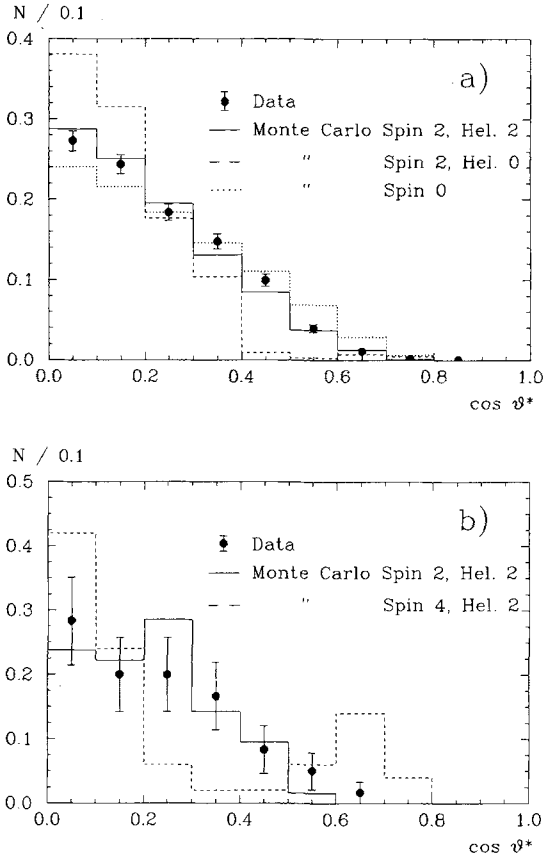

Fig. 5a, b. $\cos\vartheta^*$. ϑ^* is the polar decay angle in the $\pi^0\pi^0$ CM-system. **a** $W=1.1$–1.5 GeV/c^2 ($f_2(1270)$ region). **b** $W=1.82$–2.22 GeV/c^2 ($f_4(2050)$ *region*)

as a combination of the helicity 0 components and additional assumptions are needed in order to separate the spin 2 helicity components. In [19] the same conclusion is drawn.

In our angular analysis for reaction (2) we have chosen the region with the highest statistics. The experimental decay angle distribution* for the $f_2(1270)$ region, 1.1–1.5 GeV/c^2, is shown in Fig. 5a, together with curves from the Monte Carlo simulation of the $f_2(1270)$ resonance, under the assumption of either spin 0 or spin 2, helicity 2 and 0 production. The data are in very good agreement with the spin 2, helicity 2 simulation. However, to put a limit on the spin 2, helicity 0 contribution, an assumption has to be made concerning the presence of a spin 0 resonance contribution. The only known spin 0 resonance in this mass range is the $f_0(1400)$ [6] with a mass of $\sim$1400 MeV/c^2 and width of 150–400 MeV. Using the mass spectrum in Fig. 3, the spin 0 contribution can be conservatively limited to $<20\%$, unless the $f_0(1400)$ has a mass and width very close to that of the $f_0(1270)$. With this limitation, a fit of the data in Fig. 5a yields 100% helicity 2 for the spin 2 component. The spin 2, helicity 0 contribution is less than 15% at the 95% C.L.

This agrees with theoretical considerations [7–9] which predict strong suppression of the helicity 0 amplitude in the decay of $^3P_2$ mesons into two photons. We note that several previous experiments have also arrived at the conclusion that helicity 2 dominates in $f_2(1270)$ production [10–13], however, they assumed either that no spin 0 term is present near the $f_2(1270)$ or that the helicity 0 interference term is zero, i.e. $\delta=90°$. The latter assumption is not justified. On the contrary, δ has a considerable effect on the relative helicity contributions and the interference term cannot be neglected.

Monte Carlo simulation

In the Monte Carlo simulation of reactions (2) and (3) the generator program of [20] was used. This program performs an integration of the luminosity function, in the formulation of Bonneau et al. [21]. Only the transverse-transverse polarization component ((29d) in [21]) was considered. The $\sigma_{\gamma\gamma}$ cross section (σ_{TT} in [21]) used the Breit-Wigner parameterization in (8) for the various resonances. In addition, both virtual photons were multiplied by a ρ form-factor, $1/(1+Q^2/M_\rho^2)^2$, in the integration of the luminosity function. For the decay of the resonances, the SAGE [22] program was used. The 4-vector events generated this way were then passed through the JADE detector simulation program, which included a full shower simulation [23] for photons and electrons. The Čerenkov radiation response of the lead-glass (SF5 and SF6) was properly simulated, including the wavelength dependence of the photocathode sensitivity and the light transmission in lead glass and light guide material. Finally, the simulated events were subjected to the same selection cuts as the real events. Excellent agreement is observed between the various distributions of the real data and the corresponding distributions from the Monte Carlo simulations.

Fits of the mass distributions

The mass distributions in Figs. 3 and 4 were fitted with the expression

$$\frac{dN}{dW}=L_{e^+e^-}\int dW'\,\frac{1}{\sqrt{2\pi}\sigma_{W'}}\,e^{\frac{(W-W')^2}{2\sigma_{W'}^2}}\,\frac{d\tilde{L}_{\gamma\gamma}}{dW'}$$
$$\cdot(\varepsilon_1(W')\,\mathrm{BR}_1\,\mathrm{BW}_1+\varepsilon_2(W')\,\mathrm{BR}_2\,\mathrm{BW}_2+\mathrm{BG}). \quad (10)$$

Here N is the number of events, $L_{e^+e^-}$ is the total integrated e^+e^- luminosity and $\tilde{L}_{\gamma\gamma}$ is an approximation to the $\gamma\gamma$ luminosity function* [24]. W is the $\pi^0\pi^0$ or $\pi^0\eta$ mass and σ_W, $\varepsilon_1(W)$ and $\varepsilon_2(W)$ are the W-dependent mass resolution and efficiencies as determined from Monte Carlo studies. In the efficiency calculation, pure helicity 2 production was assumed for both $f_2(1270)$ and $a_2(1320)$. In both of the distributions two Breit-Wigner

* In the experimental distributions, θ^* is taken as the decay angle with respect to the beam axis. This is a very good approximation of the $\gamma\gamma$ axis in untagged events

* This approximation is useful for the fitting procedure. In the calculation of the $\gamma\gamma$ widths we have used the properly integrated luminosity values obtained with the generator program of [20]

Table 1. Measured $\gamma\gamma$ widths

Resonance	Number of events	$\Gamma_{\gamma\gamma}$ (keV)
$f_2(1270)$	2177 ± 47	$3.19 \pm 0.09^{-0.22}_{-0.38}$ (helicity 2)
$a_2(1320)$	85 ± 9	$1.01 \pm 0.14 \pm 0.22$ (helicity 2)
$a_0(980)$	44 ± 7	$0.28 \pm 0.04 \pm 0.10$ / BR$(a_0(980) \to \pi^0\eta)$
$f_0(975)$	60 ± 8	<0.6 (95% C.L.)
$f_4(2050)$	13 ± 4	<1.1 (95% C.L.) (C.L.) (helicity 2)

resonances BW_1 and BW_2 were fitted, namely $f_0(975)$ and $f_2(1270)$ in Fig. 3 and $a_0(980)$ and $a_2(1320)$ in Fig. 4. In the first case BR_1 and BR_2 are the branching ratios into $\pi^0\pi^0 \to \gamma\gamma\gamma\gamma$ and in the latter case the branching ratios into $\pi^0\eta \to \gamma\gamma\gamma\gamma$. The potential radius r was taken as 1 Fermi. For the background term BG a smooth curve was used, $(A + B \cdot W)\, e^{-(W-C)^2/(2D^2)}$. Interference between the Breit-Wigner resonances and the background was not considered. Due to the low statistics, Particle Data Group [6] values were used to fix the masses and widths of the $f_0(975)$, $a_0(980)$ and $a_2(1320)$. The full curves in Figs. 3 and 4 show the results of the fits. The fitted background is shown as dashed line curves. The dotted curve in Fig. 3 shows the contribution from the background and the $f_2(1270)$ alone, without the $f_0(975)$. The fit yields an $f_2(1270)$ mass and width of 1264 ± 4 MeV/c^2 and 178 ± 8 MeV respectively, in very good agreement with the world averages [6]. Thus we do not confirm a previous study [10] in which the Crystal Ball collaboration found $\sim 2\sigma$ deviations in both mass and width. A more recent study [13] with the same detector is in agreement with our measurement.

We note in this context that the potential radius, which was set to 1 Fermi in the fit, is unknown. Leaving it free in the fit of the $\pi^0\pi^0$ mass distribution leads to a value 1.0 ± 0.3 Fermi, determined mainly by the events at higher masses in the tail of the $f_2(1270)$. This result depends however on the chosen parameterization of the Breit-Wigner shape. In particular, if the shape is modified by a factor $(M_R/W)^n$ [25, 26], where n is a small number, a larger radius r is needed to match a larger exponent n, in order to reproduce the observed shape of the resonance [27].

$\gamma\gamma$ widths of the resonances

The fitted number of events and the corresponding $\gamma\gamma$ widths for the various resonances considered are given* in Table 1. The main contribution to the systematic error comes from the background parameterization**. Further sources of systematic errors are uncertainties in the detector simulation ($\approx 5\%$), the event selection (2–14%) and the e^+e^- luminosity determination (3%). Finally minor systematic contributions come from the VDM (photon form factor parameterization) and from the simulation of the $\gamma\gamma$ luminosity function.

The two previous measurements of $\Gamma_{\gamma\gamma}(f_2(1270))$ using the neutral decay mode, $f_2(1270) \to \pi^0\pi^0$, by the Crystal Ball collaboration at SPEAR [10] and at DORIS [13], are in good agreement with the present measurement. This is also true for the numerous measurements using the charged decay mode, $f_2(1270) \to \pi^+\pi^-$ [31]. Taking all values together and adding statistical and systematic errors in quadrature, the weighted mean is $\Gamma_{\gamma\gamma}(f_2(1270)) = 2.91 \pm 0.13$ keV.

The Crystal Ball collaboration has measured $\Gamma_{\gamma\gamma}(a_2(1320))$ in the decay mode $\pi^0\eta$ [32]. The value agrees well with our present result. Combining this with the measurements made using the decay $a_2(1320) \to \rho^\pm\pi^\mp$ [33], gives a weighted mean of $\Gamma_{\gamma\gamma}(a_2(1320)) = 0.96 \pm 0.09$ keV.

A discussion of the $\gamma\gamma$ widths of the tensor mesons and their interpretation in SU(3) has been given by Cooper [34]. A summary of the many theoretical predictions is found in [25].

The first measurement of the $\gamma\gamma$ decay width of the scalar meson $a_0(980)$ was reported in [32]. The value, $\Gamma_{\gamma\gamma}(a_0(980)) = 0.19 \pm 0.07^{+0.10}_{-0.07}/\mathrm{BR}(a_0 \to \pi^0\eta)$, is compatible with our measurement. The weighted mean of the two results is $\Gamma_{\gamma\gamma}(a_0(980)) = 0.24 \pm 0.08/\mathrm{BR}(a_0 \to \pi^0\eta)$ keV.

No significant evidence for the $\gamma\gamma$ coupling of the other scalar meson, the $f_0(975)$, has yet been presented. The significance of the $f_0(975)$ signal in Fig. 3 is not high, due to the uncertainties in the shape of the background and the parametrization of the $f_2(1270)$ Breit-Wigner. However, taken at face value, the number of events in Table 1 corresponds to the $\gamma\gamma$ width $\Gamma_{\gamma\gamma}(f_0(975)) = 0.42 \pm 0.06^{+0.08}_{-0.18}$ keV. Preliminary signals of similar statistical significance have been reported by the Mark II [35] and Crystal Ball [13] collaborations. The values given by these experiments are in agreement with that obtained here and a weighted mean can be tentatively formed, $\Gamma_{\gamma\gamma}(f_0(975)) = 0.31 \pm 0.10$ keV.

The $\gamma\gamma$ widths of the scalar mesons $a_0(980)$ and $f_0(975)$ have been discussed at length by Barnes [36] and Shabalin [37]. Theoretical predictions have been made from $q\bar{q}$ models as well as from a $q\bar{q}q\bar{q}$ ansatz. A particular case of the latter is the interpretation of these mesons as $K\bar{K}$ molecules. Table 4 gives a summary of the various predictions. As seen, the widths given in $q\bar{q}$ model frameworks are generally much bigger than the experimental values. This is connected with the well known difficulty of describing the observed narrow total widths of $a_0(980)$ and $f_0(975)$ in $q\bar{q}$ models. The calculations in the $q\bar{q}q\bar{q}$ framework are also uncertain. The result in [50], recalculated in [45], is an order of magnitude estimate. The $K\bar{K}$ molecule interpretation of these mesons can however explain the narrow total widths. We also note that although the branching ratio BR$(a_0 \to \pi^0\eta)$ is not known, it can be assumed to be large [6, 36] and the measured widths can thus be considered

* Previously reported preliminary results [28, 29, 30] are superseded by the present, final analysis

** This includes the systematic error coming from different Breit-Wigner parameterizations and changes of the potential radius r

to be of equal size. This is expected in the $K\bar{K}$ framework; in $q\bar{q}$ models, the $\gamma\gamma$ widths should, for ideal mixing, be related by a quark charge factor, $\Gamma_{\gamma\gamma}(f_0(975)) = 25/9 \cdot \Gamma_{\gamma\gamma}(a_0(980))$.

Analysis of $\pi^0\pi^0$ production for $m(\pi^0\pi^0) > 2$ GeV/c^2

Due to the fine granularity of the JADE lead glass calorimeter, π^0's with energies up to about 2 GeV can be efficiently reconstructed from two measured photons. This allows the study of the reaction $\gamma\gamma \to \pi^0\pi^0$ beyond the $f_2(1270)$ region. Apart from the possible resonance contribution, e.g. $f_4(2050)$ and the tail of the $f_2(1270)$, direct $\pi^0\pi^0$ production is of interest here.

There is no significant signal for $f_2(2050)$ production in Fig. 3. In principle, an upper limit to the $f_4(2050)$ cross section could be obtained from a fit to the $\pi^0\pi^0$ mass spectrum. More sensitivity is, however, obtained by considering the decay angle distribution in the $f_4(2050)$ mass region, 1.82–2.22 GeV/c^2. This distribution is shown in Fig. 5b, together with curves from the Monte Carlo simulation of $f_2(1270)$ (helicity 2) and $f_4(2050)$ production. The latter resonance is assumed to be produced in a helicity 2 state. Clearly the data are in good agreement with the spin 2, helicity 2 curve and disagree with the spin 4, helicity 2 hypothesis. The upper limit obtained from a fit to the data in Fig. 5b is given in Table 1.

A limit on $\Gamma_{\gamma\gamma}(f_4(2050))$ has been given by the TASSO collaboration [51], using the decay $f_4(2050) \to K_S^0 K_S^0$. The present measurement is much more stringent, due to the higher branching ratio of $f_4(2050)$ into $\pi\pi$. The new limit is close to the theoretical prediction given in [8] for the $\gamma\gamma$ production of the f recurrence.

For $\pi^0\pi^0$ masses higher than 2 GeV/c^2 we calculate cross sections for the angular range $|\cos\vartheta^*| < 0.3$, for which predictions from Brodsky and Lepage [1] are available. In this angular range the efficiency is approximately equal for the two helicity states as is also the case for the predicted angular distribution for direct pion pair production [1]. Using the expression

$$\frac{N_{\Delta W}}{L_{e^+e^-}\,\varepsilon_{\Delta W}(\mathrm{BR}(\pi^0 \to \gamma\gamma))^2} = \sigma_{\gamma\gamma}|_{\Delta W} \int_{\Delta W} \frac{dL_{\gamma\gamma}}{dW}\, dW, \qquad (11)$$

where ΔW is a mass interval, we arrive at the values given in Table 2 and plotted in Fig. 6. The errors are dominated by statistics and include the systematic error (added quadratically).

For completeness we give in Table 3 the cross sections obtained under the assumptions of spin 2, helicity 2 and spin 0 production mechanisms, without restrictions on the decay angle ϑ^*.

In Fig. 6 the measured cross section* for $\gamma\gamma \to \pi^+\pi^-$ [3] is also shown, multiplied by a factor $\frac{1}{2}$. The agreement with the $\pi^0\pi^0$ cross section is good, implying that the data can be explained as isospin 0 production. The

* These data points have an additional systematic error of 20% [3], not shown in the plot

Table 2. Cross sections $\sigma(\gamma\gamma \to \pi^0\pi^0)$ for $|\cos\theta^*| < 0.3$

$\pi^0\pi^0$ mass range	Number of events ($\lvert\cos\theta^*\rvert < 0.3$)	Cross section (nb)
2.0–2.1	11	1.7 ±0.5
2.1–2.2	4	0.7 ±0.4
2.2–2.3	4	0.8 ±0.4
2.3–2.5	1	0.12±0.12
2.5–3.0	2	0.11±0.08
3.0–3.5	1	0.20±0.22

Table 3. Cross sections $\sigma(\gamma\gamma \to \pi^0\pi^0)$ under assumptions of spin 2, hel. 2 and spin 0 production

$\pi^0\pi^0$ mass range	Number of events	Cross section (nb) (Spin 2, hel. 2)	Cross section (nb) (Spin 0)
2.0–2.1	15	5.7 ±1.5	4.0 ±1.0
2.1–2.2	7	2.8 ±1.1	1.8 ±0.7
2.2–2.3	5	2.2 ±1.0	1.4 ±0.6
2.3–2.4	3	1.7 ±1.0	1.2 ±0.7
2.4–2.5	1	0.55±0.55	0.38±0.38
2.5–3.0	3	0.36±0.21	0.25±0.15
3.0–3.5	1	0.22±0.22	0.16±0.16

Table 4. Theoretical predictions of $\gamma\gamma$ widths of scalar mesons

Model	Ref.	$\Gamma_{\gamma\gamma}(a_0(980))$ (keV)	$\Gamma_{\gamma\gamma}(975))$ (keV)
$q\bar{q}$	[38]	50	
$q\bar{q}$	[8]	"significant"	
$q\bar{q}$	[39]	2.5–3.8	6.9–10.6
$q\bar{q}$	[40]		0.05–0.20
$q\bar{q}$	[41]	0–0.37	
$q\bar{q}$	[42]	550±270	
$q\bar{q}$	[43]	4.8	≦14.4
$q\bar{q}$	[44]	1.3	
$q\bar{q}$	[45]	0.5	
$q\bar{q}$	[46]	~1.5	~4.5
$q\bar{q}$	[47]	0.19	0.89
$q\bar{q}$	[48]	1.6–2.6	
$q\bar{q}$	[49]	$0.6/\mathrm{BR}(a_0 \to \pi^0\eta)$	
$q\bar{q}q\bar{q}$	[50]	0.27	0.27
$q\bar{q}q\bar{q}$	[37]	1.7 or 2.2	
$q\bar{q}q\bar{q}$	[48]	"suppressed"	
$K\bar{K}$	[46]	~0.6	~0.6

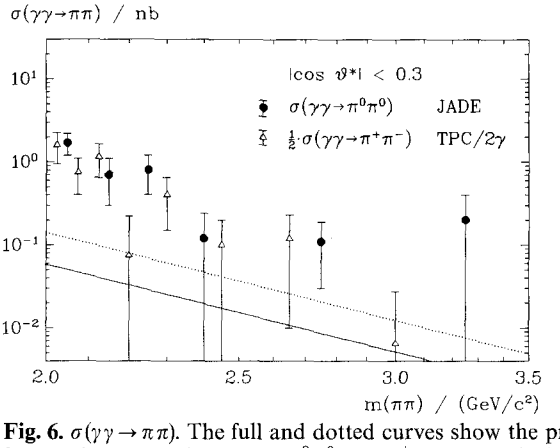

Fig. 6. $\sigma(\gamma\gamma \to \pi\pi)$. The full and dotted curves show the predictions from a QCD-calculation, for $\pi^0\pi^0$ and $\pi^+\pi^-$ respectively. The latter prediction has been multiplied by a factor 1/2

predictions from a QCD-calculation (curves (*c*) in [1]) are also shown in Fig. 6, for $\pi^0\pi^0$ (full curve) and for $\pi^+\pi^-$ (dotted curve, including the factor $\frac{1}{2}$). These predictions are an order of magnitude below the data.

Summary

In conclusion, we have studied resonance production in the reactions $\gamma\gamma \to \pi^0\pi^0$ and $\gamma\gamma \to \pi^0\eta$. Significant signals for the production of $f_0(1270)$, $a_0(980)$ and $a_2(1320)$ were observed and the $\gamma\gamma$ widths measured. The results agree well with previous measurements; in particular the measurement of $\Gamma_{\gamma\gamma}(a_0(980))$ confirms the earlier Crystal Ball measurement. Upper limits for the $\gamma\gamma$ widths of $f_0(975)$ and $f_4(2050)$ were also obtained. The widths obtained for the scalar mesons $a_0(980)$ and $f_0(975)$ support their interpretation as $K\bar{K}$ molecules, rather than normal $q\bar{q}$ resonances. The $f_2(1270)$ was found to be produced mainly in a helicity 2 state, however this conclusion could only be reached under the assumption that no significant spin 0 contribution is present under the $f_2(1270)$.

Finally the cross sections $\sigma(\gamma\gamma \to \pi^0\pi^0)$ were measured for the first time in the mass range 2–3.5 GeV/c^2. Comparison with the cross sections for the process $\gamma\gamma \to \pi^+\pi^-$ in the same mass range indicates that the production can be explained by isospin 0 contributions. The cross section for direct $\pi^0\pi^0$ production as calculated in QCD is an order of magnitude below the measurements.

Acknowledgements. We are indebted to the PETRA machine group and the DESY computer center staff for their excellent support during the experiment and to all the engineers and technicians of the collaborating institutions who have participated in the construction and maintenance of the apparatus. Helpful discussions with K.H. Karch, K. Königsmann and H. Marsiske are gratefully acknowledged. This experiment was supported by the Bundesministerium für Forschung und Technologie, by the Ministry of Education, Science and Culture of Japan, by the UK Science and Engineering Research Council through the Rutherford Appleton Laboratory and by the US Department of Energy. The visiting groups at DESY wish to thank the DESY directorate for the hospitality extended to them.

References

1. S.J. Brodsky, G.P. Lepage: Phys. Rev. D24 (1981) 1808
2. M. Benayoun, V.L. Chernyak: College de France preprint LPC 8901
3. TPC/2γ Coll. H. Aihara et al.: Phys. Rev. Lett. 57 (1986) 404
4. JADE Coll. W. Bartel et al.: Phys. Lett. 88B (1979) 171; Phys. Lett. 92B (1980) 206; Phys. Lett. 99B (1981) 277
5. V.M. Budnev, I.F. Ginzburg, G.V. Meledin, V.G. Serbo: Phys. Rep. 15 (1975) 181
6. Particle Data Group, G.P. Yost et al.: Phys. Lett. 204B (1988) 1
7. A.I. Alekseev: Sov. Phys. (JETP) 34(7) (1958) 826; M. Krammer, H. Krasemann: Phys. Lett. 73B (1978) 58; M. Krammer: Phys. Lett. 74B (1978) 361
8. B. Schrempp-Otto, F. Schrempp, T. Walsh: Phys. Lett. 36B (1971) 463 and private communication
9. P. Grassberger, R. Kögerler: Nucl. Phys. B106 (1976) 451
10. Crystal Ball Coll. C. Edwards et al.: Phys. Lett. 110B (1982) 82
11. TASSO Coll. M. Althoff et al.: Z. Phys. C – Particles and Fields 10 (1981) 117
12. DELCO Coll. A. Courau et al.: Phys. Lett. 147B (1984) 227; DELCO Coll. R. Johnson: Ph.D. Thesis, SLAC-294 (1986)
13. Crystal Ball Coll. H. Marsiske et al.: DESY Report 90-002, SLAC-PUB-5163, subm. f. publ. in Phys. Rev. D
14. J.D. Jackson: Nuovo Cimento 34 (1964) 1644
15. H. Pilkuhn: Properties and production spectra of elementary particles. Landolt and Börnstein eds., Neue Serie I/6. Berlin, Heidelberg, New York: Springer 1972
16. J.M. Blatt, V.F. Weisskopf: Theoretical nuclear physics. New York: Wiley 1952
17. F. von Hippel, C. Quigg: Phys. Rev. D5 (1972) 624
18. Proceedings of the 8th Intern. Workshop on Photon-Photon Collisions, U. Karshon, (ed.) Shoresh, Israel 1988
19. M.R. Pennington in [18, p 297]
20. S. Kawabata: Program write-Up (1982), unpubl. Contribution to the parallel sessions, reported by J.H. Field: Proceedings of the Fourth Intern. Colloquium on Photon-Photon Interactions, ed. G.W. London, Paris (1981) 447
21. G. Bonneau, M. Gourdin, F. Martin: Nucl. Phys. B54 (1973) 573
22. J. Friedman: Program Write-up, (1972) unpubl.
23. H. Messel, D.F. Crawford: Electron-photon shower distribution function tables. Oxford, New York: Pergamon 1970); A. Sato: Masters Thesis, Tokyo University (1978), unpubl.; S. Yamada, J. Olsson: Jade Notes 20 and 20a, unpubl.
24. J.H. Field: Nucl. Phys. B168 (1980) 477; Erratum: Nucl. Phys. B176 (1980) 545
25. M. Poppe: Int. J. Mod. Phys. 12 (1986) 545
26. Z.Y. Fang, G. Lopez Castro, J. Pestieau: Université Catholique de Louvain preprint UCL-IPT-87-07 (1987)
27. T. Oest: Diplomarbeit, Hamburg University 1988, unpublished
28. Jade Coll., reported by G. Heinzelmann: Proceedings of the 21st Intern. Conference on High Energy Physics. P. Petiau, M. Porneuf, (eds.) Paris 1982, p 59
29. J. Olsson: Proceedings of the Fifth Intern. Workshop on Photon Collisions, Ch. Berger (ed.), Aachen 1983, p 45
30. JADE Coll.: reported by J. Olsson in [18, p. 77]
31. PLUTO Coll. Ch. Berger et al.: Phys. Lett D54 (1980) 254; TASSO Coll.: R. Brandelik et al.: Z. Phys. C – Particles and Fields 10 (1981) 117; Mark II Coll. A. Roussarie et al.: Phys. Lett. 105B (1981) 304; Mark II Coll. J. Smith et al.: Phys. Rev. D30 (1984) 851; CELLO Coll. H.-J. Behrend et al.: Z. Phys. C – Particles and Fields 23 (1984) 223; PLUTO Coll. Ch. Berger et al.: Z. Phys. C – Particles and Fields 26 (1984) 199; DELCO Coll. A. Courau et al.: Phys. Lett. 147B (1984) 227; DELCO Coll. R. Johnson: Ph.D. Thesis, SLAC-294 (1986), TPC/2γ Coll. H. Aihara et al.: Phys. Rev. Lett. 57 (1986) 404; CELLO Coll.: reported by J. Harjes in [18, p 85]; Mark II Coll.: in [35]; TOPAZ Coll. I. Adachi et al.: Phys. Lett. 234B (1990) 185
32. Crystal Ball Coll. D. Antreasyan et al.: Phys. Rev. D33 (1986) 1847
33. CELLO Coll. H.-J. Behrend et al.: Phys. Lett. 114B (1982) 378, Erratum: Phys. Lett. 125B (1983) 518; JADE Coll.: in [29]; PLUTO Coll. Ch. Berger et al.: Phys. Lett. 149B (1984) 427; TASSO Coll. M. Althoff et al.: Z. Phys. C – Particles and Fields 31 (1986) 537; TPC/2γ Coll., reported by A. Eisner: Proceedings of the Intern. Europhysics Conf. on H.E. Physics, Uppsala, 1987; MD-1 Coll. A.E. Blinov et al.: Novosibirsk preprint 87–92 (1987); CELLO Coll. H.-J. Behrend et al.: DESY Report 89-177
34. S. Cooper: Ann. Rev. Nucl. Part. Sci. 38 (1988) 705
35. Mark II Coll.: Presented by J. Boyer in [18, p 94]
36. T. Barnes: Proceedings of the 7th Intern. Workshop on Photon-Photon Collisions, A. Courau, P. Kessler (eds.), Paris 1986, p 25
37. E.P. Shabalin: Sov. J. Nucl. Phys. 46 (1987) 485
38. A. Bramon, M. Greco: Lett. Nuovo Cimento 2 (1971) 522
39. S.B. Berger, B.T. Feld: Phys. Rev. D8 (1973) 3875
40. S. Eliezer: J. Phys. G1 (1975) 701

41. J. Babcock, J.L. Rosner: Phys. Rev. D14 (1976) 1286
42. G.K. Greenhut, G.W. Intemann: Phys. Rev. D18 (1978) 231
43. V.M. Budnev, A.E. Kaloshin: Phys. Lett. 86B (1979) 351
44. M.K. Volkov, D.V. Kreopalov: Yad. Fiz. 37 (1983) 1297
45. E.P. Shabalin: JETP Lett. 42 (1985) 135
46. T. Barnes: Phys. Lett. 165B (1985) 434
47. J. Ellis, J. Lánik: Phys. Lett. 175B (1986) 83
48. S. Narison: Phys. Lett. 175B (1986) 88
49. C.A. Dominguez, N. Paver: Z. Phys. C – Particles and Fields 39 (1988) 39
50. N.N. Achasov, S.A. Devyanin, G.N. Shestakov: Z. Phys. C – Particles and Fields 16 (1982) 55; ibid.: Phys. Lett. 108B (1982) 134; N.N. Achasov, G.N. Shestakov: Z. Phys. C – Particles and Fields 41 (1988) 309
51. TASSO Coll. M. Althoff et al.: Z. Phys. C – Particles and Fields 29 (1985) 189